

---

# Development and optimization of laser-induced breakdown spectroscopy (LIBS) for quantification of *carbon* in steel within UV/visible region

Mohamed A. Khater<sup>1,\*</sup>, Mohammed M. Babatin<sup>2</sup>, Ali M. Eid<sup>1</sup>, Abdulaziz S. Alaamer<sup>1</sup>

<sup>1</sup>Physics department, Al-Imam Mohammad Ibn Saud Islamic University (IMSIU), 22611 Riyadh, Saudi Arabia

<sup>2</sup>Mathematics department, Al-Imam Mohammad Ibn Saud Islamic University (IMSIU), 22611 Riyadh, Saudi Arabia

## Email address:

drmakhater@gmail.com (M. A. Khater), mbabatin@hotmail.com (M. M. Babatin)

## To cite this article:

Mohamed A. Khater, Mohammed M. Babatin, Ali M. Eid, Abdulaziz S. Alaamer. Development and Optimization of Laser-Induced Breakdown Spectroscopy (LIBS) for Quantification of *Carbon* in Steel within UV/Visible Region. *American Journal of Physics and Applications*.

Vol. 2, No. 6, 2014, pp. 113-117. doi: 10.11648/j.ajpa.20140206.11

---

**Abstract:** A simple bench-top laser-induced breakdown spectroscopy (LIBS) technique is investigated for the rapid detection of sufficient amount of the light element *carbon*. The plasma investigated was generated by focusing the fundamental radiation at 1064 nm of Nd:YAG laser onto low alloy steel target. The radiation emitted from the plasma was dispersed and recorded by an echelle spectrograph combined with a time-gated EMCCD detection system. Based on an extensive survey procedure, a well-resolved relatively-intense neutral *carbon* spectral line at 396.14 nm was selected, verified and used in all measurements. In addition, optimization of the main experimental parameters, namely laser energy and delay-time for integration of the detector was carried out. Furthermore, the analytical calibration curve for *carbon*, using a series of low-alloy steel standards, was constructed and corresponding analytical figures of merit were evaluated.

**Keywords:** Laser-Induced Breakdown Spectroscopy, LIBS, Quantification, Carbon, Steel, UV/Visible

---

## 1. Introduction

Light (low atomic number) elements such as carbon and sulfur play an extremely important role in determining some of the mechanical and physical properties, such as stiffness and ductility, of almost all steel products [1,2]. For many applications, it is therefore essential to keep and monitor the concentration of these elements at trace levels.

There has been very little published work concerning the direct characterization of steels for their light elements content employing spectroscopic techniques within the readily accessible UV/visible spectral region [3]. Ishibashi [4] produced very poor results in terms of sensitivity and precision using laser ablation inductively coupled plasma-mass spectroscopy (LA-ICP-MS). In another publication, a standard laboratory LIBS system was unable to detect any carbon or sulfur line emission in the steel samples investigated within the UV/visible region [5].

Accordingly, many successful investigations on measurements of light elements content in steels have been limited to the vacuum ultraviolet spectral region [6-16] for

two obvious technical reasons. Firstly, the strongest spectral lines of all light elements are emitted from their ions in this region. Secondly, there are many interference-free spectral lines of these elements, in a clear contradiction with their UV/visible counterparts, especially from the iron emission lines, the most prevalent element in the steel samples. However, the disadvantage of using these lines is air absorption in this region due to the O<sub>2</sub> Schumann-Runge band system [3]. The light collection pathway and the spectrometers must be evacuated or at least purged with inert gases (such as nitrogen or argon) in order to obtain usable signals. Moreover, optics and gratings capable of transmitting and dispersing VUV light must also be employed. This of course leads to increasing the complication level of equipment and preventing the on-line and in-situ applications of the technique.

Laser-induced breakdown spectroscopy (LIBS) is the oldest spectroscopic technique utilizing high-power laser pulses [17]. When a pulsed high-powered laser beam is focused on a

material, a short-lived (in the order of microseconds) high-temperature (a few eV) and density ( $10^{16}$ – $10^{19}$  cm<sup>-3</sup>) plasma is generated. The fundamental concept of LIBS is similar to that of conventional plasma-based methods of optical emission spectroscopy (OES): the radiation emitted from excited/ionized species in the plasma is spectrally resolved, and the individual neutral atoms and/or atomic ions in the plume are identified and quantified by their unique wavelengths and line intensities, respectively [18].

In the present work, we develop the LIBS technique in the UV/visible spectral regime to investigate the direct and rapid quantification of the light element *carbon* in low-alloy steel targets. We carry out an extensive study for selection of *carbon* spectral lines that are most relevant for low-level measurements, and optimize some important experimental parameters. Moreover, we construct the analytical calibration curve for *carbon* and realize its figures of merit.

## 2. Experimental

A schematic diagram for the LIBS system employed is shown in “Fig. 1”.

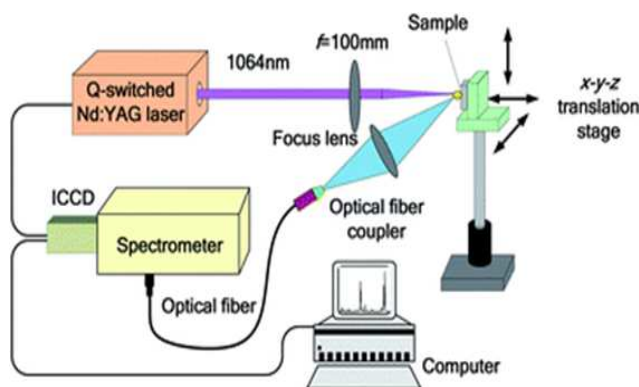


Figure 1. Experimental set-up.

A Q-switched Nd:YAG laser beam (Innolas Laser, model SpitLight Compact 400) emitting maximum pulse energy of 400 mJ at 1064 nm and 6 ns pulse width is focused onto a low alloy steel target in air at atmospheric pressure within a custom-made target chamber. The steel target is mounted on a 3-axis computer controlled translational stages with 75 mm travel and 12.5  $\mu$ m linear resolution.

The smallest radius of the laser beam waist on the steel target was calculated to be 6.0  $\mu$ m, resulting in a total laser irradiance of  $6.0 \times 10^{13}$  W/cm<sup>2</sup> at 400 mJ. The target was always kept at 1-2 mm behind the nominal focus of the laser beam in order to prevent air breakdown generation in front of the target surface, which decreases the laser-target ablation efficiency.

The radiation emitted from the laser-produced plasma is

collected by a lens and guided through an attached optical fiber cable, which is in turn connected to a 10  $\mu$ m $\times$ 30  $\mu$ m [W $\times$ H] entrance slit of an EMU-120/65 echelle spectrograph (Catalina Scientific). The spectrograph is equipped with UVU3 cassette with an aperture stop of 20 mm.

The dispersed light is then detected by an intensified front illuminated EMCCD (Andor Technology, model iXon3) with 1004 $\times$ 1002 pixel array, and 8  $\mu$ m $\times$ 8  $\mu$ m pixel size. The CCD array has a nominal quantum efficiency of 65% at 600 nm.

## 3. Results and Discussion

### 3.1. Selection of Spectral Lines

An extensive atomic data bank procedure was performed involving search and selection of spectral lines of greatest promise for low level detection in the UV/visible region of the light element *carbon*. The atomic data bank for this element and its ions includes all relevant spectrum line wavelengths, associated energy levels, oscillator strengths and possible coincidences with other spectrum lines (Using e.g. National Institute of Science and Technology (NIST), Harvard and Oak Ridge Atomic Databases and papers in the open literature).

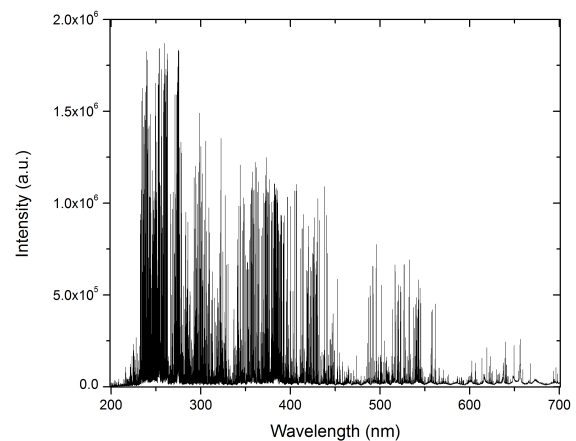


Figure 2. UV/visible spectrum of laser-produced steel plasma.

Figure 2 illustrates the UV/visible spectrum of laser-produced steel plasmas recorded at the optimum experimental conditions discussed later, using the set-up described in the previous section. As can be noted from the figure, the spectrum is naturally dominated by intense neutral as well as singly ionized Fe spectral lines.

Despite considerable efforts, we could only identify and verify a single well-isolated spectral line for the element *carbon* that is suitable for quantification; this is the neutral CI at 396.14 nm. Relevant atomic information of this spectral line is depicted in Table 1.

Table 1. Atomic data for the carbon line selected

Line [nm]	Species	I (rel.)	Energy [eV] lower - upper	Transition	Quantum number
396.1403	C I	8	7.68 - 10.81	3s1P-6p1D	1 - 2

In addition, Figure 3 shows parts of the laser-produced steel plasma spectrum in which the relative intensities of the CI 396.14 nm spectral line from two low alloy steel targets containing largest (black spectrum) and smallest (red spectrum) carbon concentrations are compared.

**3.2. Laser Energy Optimization**

In this part, the effect of laser pulse energy recorded on the emission characteristics of laser-ablated steel plasmas in air at atmospheric pressure was investigated. The laser energy was varied from about 50mJ to about 350 mJ by simply changing the delay time between flash lamps and Q-switch onsets. The remaining other conditions of both the laser and the rest of the experiment were kept constant.

Figure 4 describes the dependence of the intensity as well as background intensity of the CI 396.14 nm line on the laser pulse energy.

As expected, and can be seen from the figure, both intensities are increasing functions of the pulse energy in the range studied. However, the increase in line intensity was more pronounced in the energy range ~ 150-250 mJ. As the laser energy absorbed increases, the plasma excitation temperature as well as its electron density increases correspondingly.

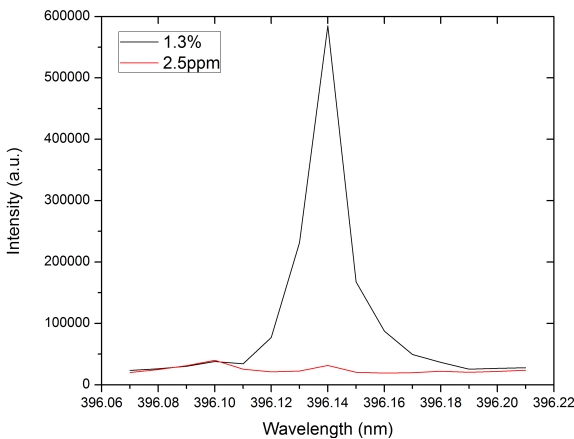


Figure 3. Relative intensities of CI 396.14 nm spectral line at maximum (black) and minimum (red) concentrations.

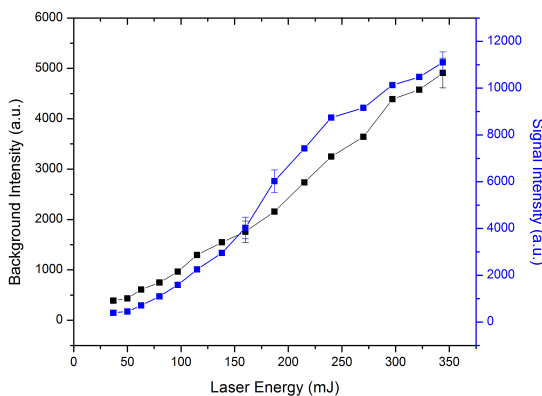


Figure 4. Dependence of CI 396.14 nm relative intensities on laser energy.

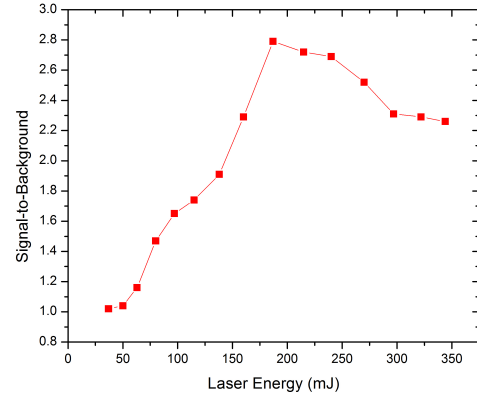


Figure 5. Dependence of CI 396.14 nm signal-to-background ratio on laser energy.

Signal-to-background ratios (calculated from measurements recorded in the previous figure) of the CI 396.14 nm are plotted versus the laser pulse energy and demonstrated in Fig. 5. It is obvious from the graph that the optimum laser energy value may be located between 160 and 190 mJ. For the rest of experiments, laser pulse energy of 175 mJ is selected.

**3.3. Detector Delay Time for Integration**

The shutter delay time of the EMCCD detector was changed from 10ns up to 5000 ns with respect to the firing onset of the laser pulse. Other conditions of the experiment were kept constant. The variation of relative intensities of the CI 396.14 nm spectral line is shown in “Fig. 6”.

The background intensity was leveled off in the range 0-1000 ns before it undergoes a significant reduction at 1250 ns and then gradually decreases up to 5000 ns. On the other hand, however, the behavior of line intensity was quite different. After being more or less stable in the 0-1000 ns range, the line intensity gradually decreased up to a delay value of about 2500 ns, and then levels off again up to about 3500 ns. Afterwards, the intensity slightly rises up to 4000 ns before it gradually declines.

Accordingly, the signal-to-background ratio of the CI 396.14 nm line gradually rises from about 1000 ns up to 4000 ns, and then levels off during the rest of the range. Although at lower values, signal-to-background ratios in the range 2500 ns to 3500 ns seem to be more relevant. A delay time of 3000 ns, therefore, was selected as the optimum value for this study because, again, the unacceptable measurement error levels at higher delay times. Figure 7 depicts the corresponding results obtained.

**3.4. Analytical Calibration Curve**

Series standards of low alloy steel alloy targets containing various concentrations of the element carbon are employed in order to inspect the linear relationship between different carbon proportions.

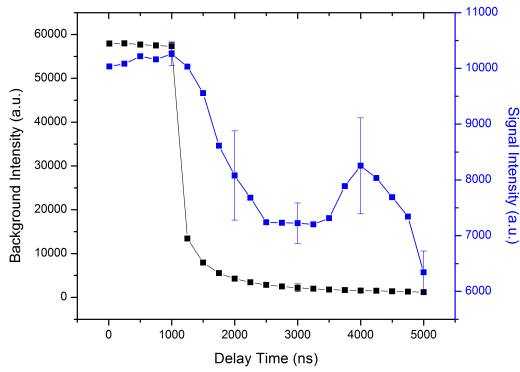


Figure 6. Dependence of CI 396.14 nm relative intensities nm on delay time of the detector.

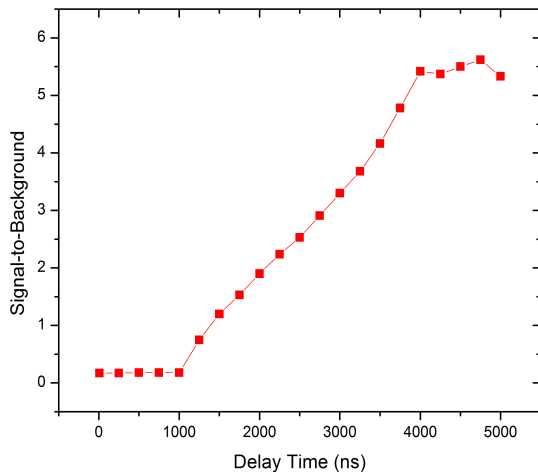


Figure 7. Dependence of CI 396.14 nm signal-to-background ratio on delay time of the detector.

We used the optimum operating conditions obtained in the previous experiments and introduced the targets to the laser pulses in succession so that measurements repeated from each target are recorded at different time intervals to ensure that they are subjected to the same conditions, especially those related to fluctuations in the laser energy. All intensity measurements throughout this work were performed by integrating the area under the spectral curve for a specific spectral interval.

Figure 8 illustrates the linear fitting for data points representing the relationship between different concentrations and corresponding integrated intensities for the CI 396.14 nm spectral line. The  $R^2$  factor of the linear fitting is about 0.98.

Precision is a measure of the dispersion of the results around a central point represented by the mean value of the measurements. It is usually calculated as the relative standard deviation (RSD) of a number of measurements:  $RSD (\%) = 100 [SD/Mean]$ , where  $SD$  is the standard deviation of the measurements.

The precision calculated, averaged over the 8 *carbon* concentration values used to construct the above calibration curve, was estimated at about 5.0%.

Accuracy is a measure of the difference between a measured concentration to the actual concentration. It is expressed as the relative error of the measurements, and is

often expressed as a percentage. For the mean value of a set of measurements it can be calculated as:  $\%Error = [100(Mean-Actual Concentration)/Actual Concentration]$ .

The average accuracy for concentration measurements was evaluated at about 8%.

Finally, the limit of detection (LOD) is a statistical measure of the minimum concentration of an element that the method could detect. It is common to describe LOD as follows:  $LOD = 3SDB_{blank}/m$ , where  $SDB_{blank}$  is the standard deviation of the intensity obtained for a sample which does not contain the element of interest (commonly known as the blank) and  $m$  is the slope of the calibration plot.

In the current experiment, a low alloy steel target containing 2.5 ppm *carbon* was selected to calculate LOD. A limit of detection of about 67 ppm was estimated for *carbon* using the CI 396.14 nm spectral line.

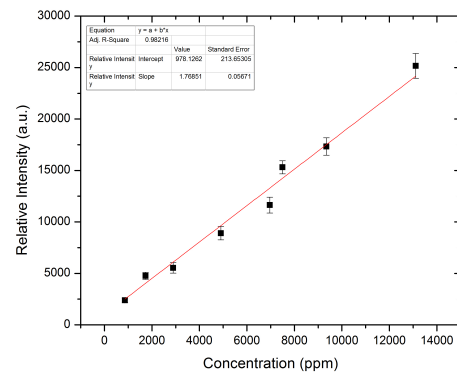


Figure 8. Analytical calibration curve for carbon in steel.

### 4. Conclusion

We developed LIBS technique in the UV/visible spectral regime to investigate the direct and rapid quantification of the light element *carbon* in low-alloy steel targets. An extensive study for selection of *carbon* spectral lines that are most relevant for low-level measurements was carried out. Moreover, we optimized some important experimental parameters including laser energy and delay-time for integration. Furthermore, a linear calibration curve for *carbon* in steel was obtained. Moreover, analytical figures namely precision, accuracy as well as detection limits were calculated at 5%, 8%, and 67 ppm, respectively.

### Acknowledgments

The authors would like to express their sincere gratitude to King Abdulaziz City for Science and Technology (KACST) for financial support through the National Science, Technology and Innovation Plan (NSTIP) program.

### References

[1] P. Harvey (Ed.), Engineering properties of steel, American Society for Metals, Ohio, 1982.

- [2] ASM Handbook Volume 01: Properties and Selection: Irons, Steels, and High-Performance Alloys; Publisher: ASM; Publication Date: 1990.
- [3] M A Khater, Laser-Induced Breakdown Spectroscopy (LIBS) for Light Elements Detection in Steel: State of the Art (invited review), *Spectrochim. Acta Part B* 81 (2013) 1–10.
- [4] Y. Ishibashi, Rapid Analysis of Steel by Inductively Coupled Plasma-Atomic Emission Spectrometry and Mass Spectrometry with Laser Ablation Solid Sampling, *ISIJ Int.* 37 (1997) 885–891.
- [5] F. De Lucia, Jr., J. Gottfried, A. Miziolek, Analysis of Carbon and Sulfur in Steel Samples Using Bench Top Laser-Induced Breakdown Spectroscopy (LIBS), General Books LLC, 2011.
- [6] J. Aguilera, C. Aragon, J. Campos, Determination of Carbon Content in Steel Using Laser-Induced Breakdown Spectroscopy. *Appl. Spectrosc.* 46 (1992) 1382–1387.
- [7] R. Sattmann, V. Sturm, R. Noll, Laser-Induced Breakdown Spectroscopy of Steel Samples Using Multiple Q-Switch Nd:YAG Laser Pulses, *J. Phys. D: Appl. Phys.* 28 (1995) 2181–2187.
- [8] A. Gonzalez, M. Ortiz, and J. Campos, Determination of Sulfur Content in Steel by Laser-Produced Plasma Atomic Emission Spectroscopy, *Appl. Spectrosc.* 49 (1995) 1632–1635.
- [9] V. Sturm, L. Peter, R. Noll, Steel Analysis with Laser-Induced Breakdown Spectrometry in the Vacuum Ultraviolet, *Appl. Spectrosc.* 54 (2000) 1275–1278.
- [10] M. Khater, P. van Kampen, J. Costello, J-P. Mosnier, E. Kennedy, Time-integrated laser-induced plasma spectroscopy in the vacuum ultraviolet for the quantitative elemental characterization of steel alloys, *J. Phys. D: Appl. Phys.* 33 (2000) 2252–2262.
- [11] M. Hemmerlin, R. Meilland, H. Falk, P. Wintjens, L. Paulard, Application of Vacuum Ultraviolet Laser-Induced Breakdown Spectrometry for Steel Analysis — Comparison with Spark-Optical Emission Spectrometry Figures of Merit. *Spectrochim. Acta B* 56 (2001), 661–669.
- [12] M. Khater, J. Costello, E. Kennedy, Optimization of the Emission Characteristics of Laser-Produced Steel Plasmas in the Vacuum Ultraviolet: Significant Improvements in Carbon Detection Limits, *Appl. Spectrosc.* 56 (2002) 970–983.
- [13] L. Peter, V. Sturm, R. Noll, Liquid Steel Analysis with Laser-Induced Breakdown Spectrometry in the Vacuum Ultraviolet, *Appl. Opt.* 42 (2003) 6199–6204.
- [14] I. Radivojevic, C. Haisch, R. Niessner, S. Florek, H. Becker-Ross, U. Panne, Microanalysis by Laser-Induced Plasma Spectroscopy in the Vacuum Ultraviolet, *Anal. Chem.* 76 (2004) 1648–1656.
- [15] M. Khater, Application of Laser-ablated Plasmas to Compositional Analysis of Steel in the Vacuum Ultraviolet, *J. Kor. Phys. Soc.* 58 (2011) 1581–1586.
- [16] M. Khater, Spatial characteristics of vacuum UV emission from laser-induced plumes in air, *Appl. Surf. Sci.* 286 (2013) 156–160.
- [17] D. Hahn, N. Omenetto, Laser-Induced Breakdown Spectroscopy (LIBS), Part II: Review of Instrumental and Methodological Approaches to Material Analysis and Applications to Different Fields, *Appl. Spectrosc.* 66 (2012) 347–419.
- [18] R. Noll, Laser-Induced Breakdown Spectroscopy: Fundamentals and Applications, first ed., Springer-Verlag, Berlin, 2012.